Chinese Science Bulletin

Fluorescence and sensitization performance of phenylene-vinylene-substituted polythiophene

CHEN JinMao[1,3], HOU JianHui[2,3], LI YongFang[2], ZHOU XiaoWen[1], ZHANG JingBo[1], LI XuePing[1], XIAO XuRui[1] & LIN Yuan[1†]

[1] Beijing National Laboratory for Molecular Sciences, Key Laboratory of Photochemistry, Center for Molecular Sciences, Institute of Chemistry, Chinese Academy of Sciences, Beijing 100190, China;
[2] Beijing National Laboratory for Molecular Sciences, Key Laboratory of Organic Solids, Center for Molecular Science, Institute of Chemistry, Chinese Academy of Sciences, Beijing 100190, China;
[3] Graduate University of Chinese Academy of Sciences, Beijing 100190, China

A new kind of polythiophene derivative, Poly(3-{2-[4-(2-ethylhexyloxy)-phenyl]-vinyl}-2,2′-bithiophene) (PTh), was applied in dye-sensitized solar cell to extend the light response of nanocrystalline TiO_2 electrode. UV-vis absorption and fluorescence spectra were employed to investigate the interaction of PTh with nanocrystalline TiO_2. The absorption coefficient of the PTh was high in visible part of spectrum, and the fluorescence emission of the PTh can be efficiently quenched by TiO_2 nanoparticles owing to charge injection from the excited singlet state of PTh to the conduction band of the TiO_2 particles. Cyclic voltammetry measurements were performed to study the dye regeneration reaction at the nanocrystalline TiO_2/electrolyte interface. The solar cell sensitized with PTh exhibited a short-circuit photocurrent (I_{sc}) of 3.08 mA/cm^2, an open circuit voltage (V_{oc}) of 511 mV and an overall efficiency of 0.9% under the illumination of 100 mW/cm^2 (AM 1.5).

polythiophene derivative, sensitize, solar cell, efficiency

Regenerative photoelectrochemical cells, also known as dye sensitized solar cells (DSSC), have attracted widespread attentions due to their high energy conversion efficiencies and low production costs[1–3]. Up to now, the most efficient dyes of the solar cell are ruthenium polypyridyl complexes[4]. Because of the problems such as high cost, long-term unavailability, undesirable environmental impact of these noble metal complexes, there remains the need for alternative photosensitizers.

Polythiophene and its derivatives, as a kind of noble metal free organic dyes, are environmentally friendly and cost comparatively less. Besides, they have many advantages, for instance their syntheses are simple and their electronic properties can easily be tuned by chemical modification[5–8]. Because of their good film forming and optical properties, thiophene-based conjugated polymers exhibit considerable performance in polymer solar cells, whose power conversion efficiency reached 3%—4% under AM 1.5 (AM=air mass) irradiation[9–12].

Among the various properties of thiophene-based conjugated polymers, the outstanding characteristics are the high absorption coefficient and wide absorption wavelength in the visible part of the spectrum, which allow a thinner nanocrystalline film to harvest the incident light efficiently in dye-sensitized solar cells. Considering the good performance in polymer solar cells and the efficient light harvesting properties, thiophene- based conjugated polymers are promising light sensitizers for application in dye-sensitized solar cells.

Recently, a novel phenylene-vinylene-substituted

Received March 11, 2008; accepted June 7, 2008
doi: 10.1007/s11434-009-0209-0
†Corresponding author (email: linyuan@iccas.ac.cn)
Supported by the Major State Basic Research Development Program of China (Grant No. 2006CB202605), High-Tech Research and Development of China Program (Grant No. 2007AA05Z439), National Natural Science Foundation of China (Grant No. 50221201), and Innovative Foundation of the Center for Molecular Science, Chinese Academy of Sciences (Grant No. CMS-CX200718)

Citation: Chen J M, Hou J H, Li Y F, et al. Fluorescence and sensitization performance of phenylene-vinylene-substituted polythiophene. Chinese Sci Bull, 2009, 54(10): 1669-1676, doi: 10.1007/s11434-009-0209-0

polythiophene, Poly(3-{2-[4-(2-ethylhexyloxy)-phenyl]-vinyl}-2,2′-bithiophene) (PTh), was synthesized and exhibited a strong and broad absorption in the visible region from 380 to 650 nm. In this paper, we adopt the present polythiophene as photosensitizer to investigate the spectrum response on the surface of TiO_2 and the mechanism of the interfacial electron injection process from excited PTh to conduction band of TiO_2. Quenching of the fluorescence emission and changes in the fluorescence lifetime of PTh afforded useful information of the process of electron transfer. The DSSC fabricated with PTh-sensitized TiO_2 electrode exhibited a considerable energy conversion efficiency and a promising potential for performance improving.

1 Experimental

1.1 Synthesis of Poly(3-(phenylenevinyl)thiophene) with conjugated side chains

Poly(3-{2-[4-(2-ethylhexyloxy)-phenyl]-vinyl}-2,2′-bithiophene) (PTh) was synthesized according to a method described elsewhere[13]. Synthetic routes of the conjugated polymer are shown in Scheme 1.

^{1}HNMR measurement was used to confirm the formation of the phenylene-vinylene-substituted polythiophene. Molecular weight and polydispersity of the polymer were determined by gel permeation chromatography (GPC) in THF on the basis of polystyrene calibration. The molecular weight of PTh was M_n=54 K with a polydispersity index of 2.3. The highest occupied molecular orbital (HOMO) and the lowest unoccupied molecular orbital (LUMO) of the polymer were calculated using cyclic voltammetry measurement.

1.2 Preparation TiO_2 colloidal and sensitization of TiO_2 electrode

The TiO_2 colloidal was synthesized by sol-gel and hydrothermal techniques from titanium isopropoxide (Aldrich, 97%) precursor. Titanium isopropoxide hydrolyzed in pH 2 aqueous solution under strong stirring at 80℃ and then autoclaved at 250℃. After ultrasonic dispersion and evaporation under vigorous stirring at 120℃, a homogeneous 12% (wt%) TiO_2 colloidal suspension was obtained. Prior to the film deposition, 10% (wt%) of monodisperse polystyrene spherical particles (200 nm in diameter) was added.

For fabricating the DSSC, the fluorine-doped tin oxide (FTO) conductive glass sheets (10 Ω/square) were washed repeatedly with detergent, then treated with ultrasonic washing and rinsed with copiously double-distilled water. The conductive glass was preserved in isopropyl alcohol before use.

The working electrode was prepared by spreading the above colloidal TiO_2 paste on FTO glass by doctor blade method using a glass rod and adhesive tape spacers. After TiO_2 film was dried in air for a few minutes, the electrode was sintered at 450℃ for half an hour in air. During this procedure, polystyrene particles were re-

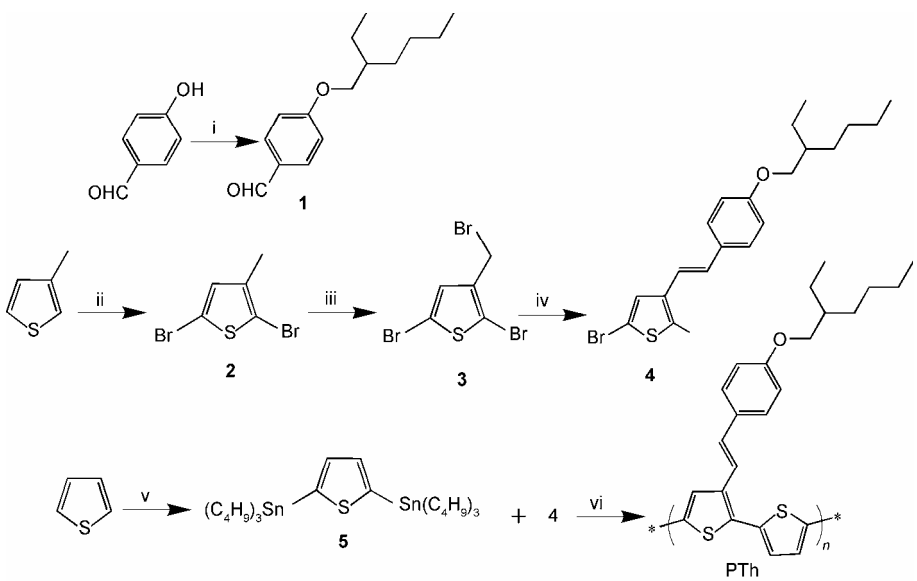

Scheme 1 Synthesis of Poly(3-{2-[4-(2-ethylhexyloxy)-phenyl]-vinyl}-2,2′-bithiophene). (i) $BrCH_2CH(C_2H_5)(CH_2)_3CH_3$, K_2CO_3, DMF, reflux, 4 h; (ii) NBS, CH_3Cl/HOAc, 2 h; (iii) NBS, BPO, CCl_4, reflux, 3 h; (iv) $P(OC_2H_5)_3$, 160°C, 2 h; then 1, $NaOCH_3$, DMF, 20°C, 30 min; (v) *n*-butyllithium, THF, reflux, 1 h; then $(C_4H_9)_3SnCl$, r. t., overnight; (vi) $Pd(PPh_3)_4$, toluene, Ar, reflux, 12 h.

moved, pores were left in the electrode, and the nanocrystalline TiO_2 electrode containing large size pores was obtained. TiO_2 nanocrystalline particles in anatase interconnected to construct a three-demensional network structure and had an average diameter of 35 nm obtained from scanning electron microscopy.

As for sensitization procedure, the prepared electrode with large size pores is in favor of adsorbing and penetration of PTh sensitizer because the size of PTh molecule is larger than the conventional *cis*-di(thiocyanato)-*N*,*N*′-bis(2,2′-bipyridyl-4,4′-dicarboxylic acid) ruthenium (II) complex ($[RuL_2(NCS)_2]$) (N3) dye, and the penetration of PTh into the pores among the TiO_2 particles is difficult than that of N3 dye. The surface morphology of the prepared nanocrystalline TiO_2 electrode is illustrated in Figure 1.

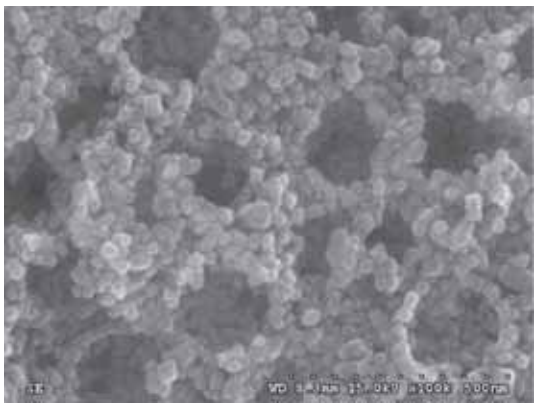

Figure 1 Surface morphologic image of the nanocrystalline TiO_2 porous film.

The adsorption of PTh on TiO_2 surface was performed by soaking the nanocrystalline TiO_2 electrode in chloroform solution of PTh in dark. The molecule size of PTh was relatively large compared with N3 dye, so the soaking time of PTh was 48 h, longer than that of N3 dye (12 h). The comparatively long adsorption time was in order to allow a high degree of penetration of the PTh into the nanostructured TiO_2. Compared with the concentration of PTh, the optimizing of soaking time of electrode was more important. In the condition of 5×10^{-4} mol/L of PTh (in the same order as N3 dye concentration), 48 h was the optimum soaking time. It was multilayer adsorption of the polythiophene adsorbed on the TiO_2 according to the calculation based on the aftermentioned surface concentration (2.0×10^{-9} mol/cm^2).

1.3 Measurements

Scanning electron microscopy (Hitachi-S-4300) was employed to study the surface morphologies of TiO_2 electrodes.

Absorption spectra were taken on a SHIMADZU UV-1601 UV-vis spectrophotometer (190—1100 nm range).

The steady state fluorescence spectra were measured using a Hitachi F-4500 spectrophotometer (200—800 nm range).

The fluorescence lifetime measurements were carried out on a multiplexed, time-correlated, single-photon counting spectrofluorometer (Edinburgh FLS-920), excited using the pulsed light of a hydrogen lamp. Fluorescence lifetimes from picoseconds to several hundred microseconds could be accurately recorded with this spectrofluorometer.

The morphology of the TiO_2 electrode was detected by a field emission scanning electron microscopy (SEM) (Hitachi S-4300 model).

Photovoltaic measurements were performed with a potentiostat/galvanostat (EG&G Princeton Applied Research, model 273) under simulated AM1.5 irradiation with an incident power density of 100 mW/cm^2 using a 300-W Xe arc lamp solar simulator (Oriel instrument USA 961160-1000). The operation was conducted at room temperature and the active cell area was 0.20 cm^2.

2 Results and discussion

2.1 Absorption spectrum

Figure 2 curve 1 shows the absorption spectrum of PTh in chloroform solution. The PTh sensitizer shows two maximum absorption peaks: one in visible region is attributed to the π-π* transition of the conjugated polymer main chains, the other in the UV region is attributed to the conjugated side chains.

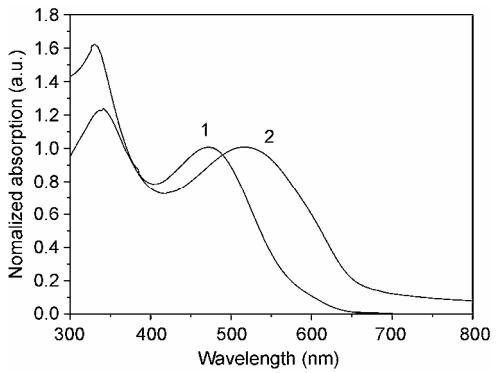

Figure 2 Absorption spectra of PTh solution in chloroform (curve 1) and PTh film spin-coated (curve 2) from chloroform solution.

From the absorption spectrum, we can calculate the adsorption coefficient at maximum absorption (ε = 2.5×10^5 L·mol^{-1}·cm^{-1}, 471 nm), which is higher than that of N3 dye (1.4×10^4 L·mol^{-1}·cm^{-1}, 518 nm). The strong absorption in the visible region makes PTh good candidate become the sensitizer of large band-gap semiconductor materials such as TiO_2.

In comparison with the absorption spectra of the PTh solutions, the visible absorption peaks of PTh film (Figure 2, curve 2) red-shifted by 45 nm. The red-shift of the π-π* transition of the PTh film should be due to the strong interaction between the PTh chains in the solid film.

As shown in Figure 3, adding 1.87×10^{-3} mol/L TiO_2 suspension into the above PTh chloroform solution, no wavelength shift with respect to the pure PTh is observed. Combining the results of steady-state fluorescence in Figure 4(a), we can conclude that no charge transfer bands or significant electronic interaction occur between the two components in ground-state or any emissive exciplex formation may be ruled out.

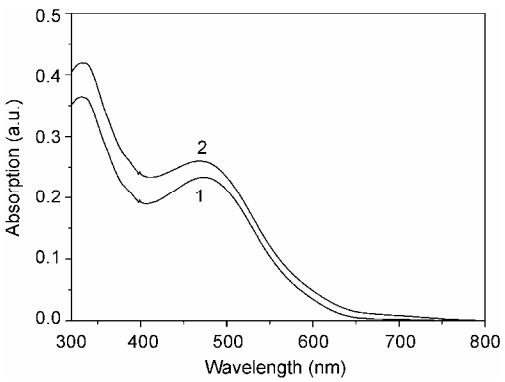

Figure 3 Absorption spectrum of 1.0×10^{-5} g/mL PTh in chloroform (curve 1) in the absence and (curve 2) in presence of 1.87×10^{-3} mol/L TiO_2 suspension.

2.2 Steady-state fluorescence spectrum

Solutions of PTh with TiO_2 nanocrystals were studied by fluorescence as a function of the concentration of nanocrystals. As illustrated in Figure 4(a), the fluorescence yield decreased upon successive addition of TiO_2 nanoparticles to a solution of 1.0×10^{-5} g/mL PTh in chloroform.

The fluorescence emission quenching can be attributed to electron transfer or energy transfer from the excited singlet state of PTh to the TiO_2 particles. Because the excitation energy of polythiophene PTh is relatively low (long wavelength excitation), it is not high enough for transferring the energy to TiO_2. So the mechanism of energy transfer can not be responsible for the fluorescence quenching of PTh by TiO_2 particles, which is caused by electron transfer.

As for PTh films (Figure 4(b)), the quenching of the fluorescence for PTh coated on TiO_2 electrode was obvious and was also attributed to efficient electron transfer from PTh the TiO_2.

In order to verify the above conclusion, we calculated and compared the relative energy levels of the excited singlet state of the PTh molecules and the conduction band of TiO_2. From the onset oxidation potentials (E_{ox}) and the onset reduction potentials (E_{red}) of the PTh, HOMO and LUMO energy levels as well as the energy gap of the PTh were calculated according to the following equations[13]:

$$\text{HOMO} = -e(E_{ox} + 4.71)\ \text{(eV)}, \quad (1)$$

$$\text{LUMO} = -e(E_{red} + 4.71)\ \text{(eV)}, \quad (2)$$

$$E_g = e(E_{ox} - E_{red})\ \text{(eV)}, \quad (3)$$

where the units of E_{ox} and E_{red} are V vs. Ag/Ag^+.

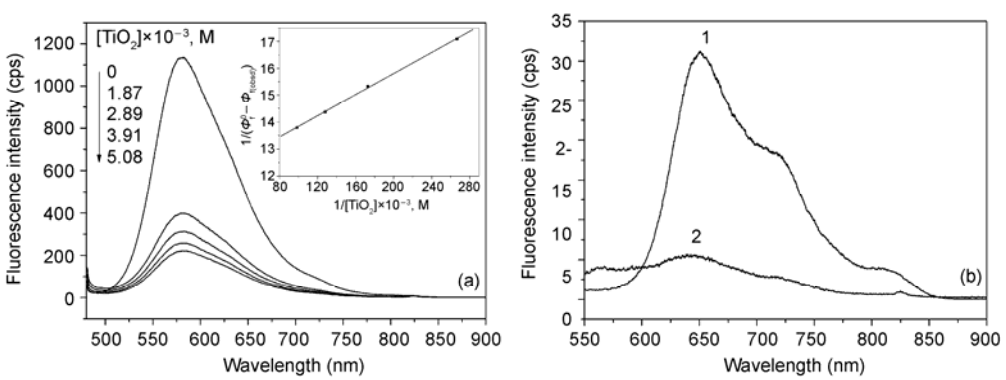

Figure 4 Fluorescence quenching of PTh. (a) Fluorescence quenching of 1.0×10^{-5} g/mL PTh chloroform solution at various TiO_2 concentrations (λ_{ex} = 471 nm). Insert shows the dependence of $1/(\Phi_f^0-\Phi_{f(obsd)})$ on the reciprocal concentration of TiO_2 suspension; (b) fluorescence quenching of PTh film on the surface of TiO_2 electrode (curve 1, coated on glass slide and curve 2, coated on TiO_2 electrode).

On the basis of the relative positions of PTh and TiO_2 energy levels shown in Figure 5, the electron injection would be thermodynamically allowed from the from the excited singlet of the PTh to the conduction band of TiO_2.

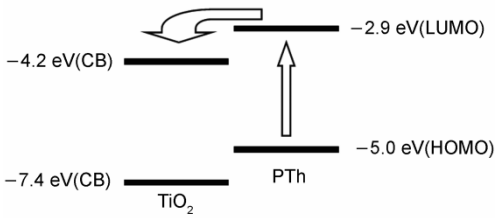

Figure 5 Schematic energy level of and photoinduced charge transfer at PTh/TiO_2 nanoparticles interface. The vacuum level is defined at 0 eV.

The participation of TiO_2 in the quenching process was further investigated by considering the equilibrium between adsorbed and unadsorbed molecules of PTh sensitizer with an apparent association constant of K_{app}[14].

$$\mathrm{PTh}+\mathrm{TiO_2} \xleftrightarrow{K_{app}} [\mathrm{PTh}\cdots\mathrm{TiO_2}]. \quad (4)$$

The observed quantum yield ($\Phi_{f(obsd)}$) of the PTh in a TiO_2 nanoparticles suspension can be related to the fluorescence yields of unadsorbed (Φ_f^0) and adsorbed (Φ_f') molecules of the PTh sensitizer by the following equation

$$\phi_f(\mathrm{obsd}) = (1-\alpha)\phi_f^0 + \alpha\phi_f', \quad (5)$$

where α is the degree of association between TiO_2 and PTh sensitizer. At relatively high TiO_2 concentrations ($[\mathrm{TiO_2}] >> [\mathrm{PTh}]$), the expression of α can be written as

$$\alpha = \frac{K_{app}[\mathrm{TiO_2}]}{1+K_{app}[\mathrm{TiO_2}]}. \quad (6)$$

By substituting the value of α in eq. (5). Eq. (5) could be simplified to

$$\frac{1}{\phi_f^0-\phi_f(\mathrm{obsd})} = \frac{1}{\phi_f^0-\phi_f'} + \frac{1}{K_{app}(\phi_f^0-\phi_f')[\mathrm{TiO_2}]}. \quad (7)$$

As we can see from eq. (7), there was a linear dependence of $1/(\Phi_f^0-\Phi_{f(obsd)})$ on the reciprocal concentration of TiO_2 suspension and a slope equal to $1/(K_{app}(\Phi_f^0-\Phi_f'))$ (insert in Figure 4(a) insert). We can calculate the value of K_{app} (606 mol/L^{-1}). For PTh, each main chain has about one hundred monomer units, so the K_{app} is considered large, suggesting that there was a relatively strong complex interaction between PTh molecules and TiO_2 nanoparticles.

2.3 Time-resolved fluorescence spectrum

In order to probe the mechanism of fluorescence quenching process of PTh by TiO_2 nanoparticles, fluorescence lifetime measurements were performed.

In neat chloroform, the fluorescence of PTh exhibited a single-exponential decay (Fit=$A+B_1\exp(-t/\tau_1)$) with a lifetime of 0.54 ns. In the presence of TiO_2 suspension, however, it deviated from a single-exponential decay. The fluorescence decay for PTh in TiO_2 suspension is shown in Figure 6. The fluorescence fitted a two-exponential decay (Fit=$A+B_1\exp(-t/\tau_1)+B_2\exp(-t/\tau_2)$). There was an obvious component with a much shorter lifetime. A component with a lifetime similar to that of PTh alone in chloroform was also observed. The fluorescence lifetimes of the two components attributed to PTh adsorbed on TiO_2 nanoparticles and unadsorbed PTh were 0.17 and 0.61 ns respectively. From the above analyses, it is indicated that the fluorescence quenching process of PTh by TiO_2 suspension was static due to the adsorption of PTh on TiO_2 particles, being in agreement with the quenching model proposed by Kamat[14] The detailed data of time-resolved fluorescence are listed in Table 1.

The observed decrease in the singlet lifetime of PTh parallels the fluorescence quenching experiments described earlier and supports the involvement of the

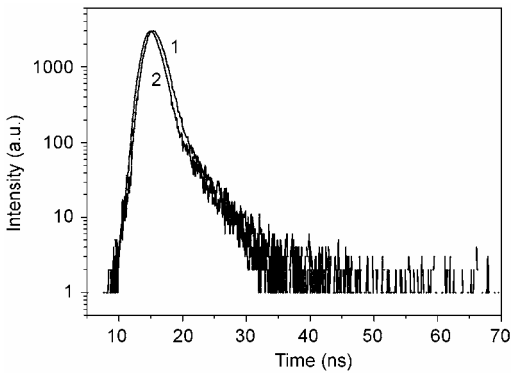

Figure 6 Fluorescence decay and normalized instrument response curves for 1.0×10^{-5} g/mL in 1.8×10^{-3} mol/L TiO_2/chloroform suspension. The excitation wavelength was at 471 nm, and the fluorescence emission was recorded at 584 nm. Curve 1 is the fluorescence decay curve fit to a two-exponential decay law and curve 2 is the instrument response.

Table 1 Fluorescence lifetime measurement for PTh

$[TiO_2]$ (mol/L)	A	B	τ (ns)	χ^2
0	0.86	B_1=0.21	τ_1=0.54 (100%)	1.03
1.8×10^{-3}	0.61	B_1=0.09 B_2=0.30	τ_1=0.17 (47.05%) τ_2=0.61 (52.95%)	1.19

λ_{ex} = 471nm, λ_{em} = 584 nm, [PTh] = 1.0×10^{-5} g/mL

charge-transfer step (K_{et}) in the quenching process:

$$PTh^{*}(S1)+TiO_2 \xrightarrow{K_{et}} PTh^{+\cdot}+TiO_2(e_{cb}^{-}) \quad (8)$$

The rate constant of electron transfer from the excited singlet state of PTh to the conduction band of TiO_2 would be given by Kamat[15]

$$K_{et}=\frac{1}{\tau_{ads}}-\frac{1}{\tau}, \quad (9)$$

where τ and τ_{ads} are the lifetimes of the sensitizer in chloroform and adsorbed onto the TiO_2 surface. The value of K_{et} obtained upon substitution of the values of τ (0.61 ns) and τ_{ads} (0.17 ns) in eq. (9) is 4.24×10^{9} s^{-1}. The variation in the solvent environment and the energetics of the excited sensitizer is expected to influence the specific rate of the charge injection process.

The quantum yield of charge injection from PTh to TiO_2 is given by

$$\phi_{inj}=\frac{K_{et}}{\tau^{-1}+K_{et}}, \quad (10)$$

where K_{et} is the above-mentioned rate constant for electron injection and τ is the excited-state lifetime in the absence of injection. Using $K_{et}=4.24\times10^{9}$ s^{-1} and $\tau=0.54$ ns, we can obtain $\phi_{inj}=0.69$.

2.4 Photosensitization of PTh on nanocrystalline TiO_2 electrode

The nanocrystalline TiO_2 electrode was sensitized by PTh in the following way: after heating at 100℃ for about one hour, the TiO_2 electrode was immersed in 5×10^{-4} mol/L PTh chloroform solution for 48 h under dark. The comparatively long adsorption time was in order to allow a high degree of penetration of the PTh into the nanostructure TiO_2. The absorption spectrum of the sensitized electrode was also measured. The amount of PTh adsorbed on TiO_2 surface can be calculated through the absorption spectrum, which is about 2.0×10^{-9} mol/cm^2.

In order to study the effect of expending the visible light response of large-band gap semiconductor TiO_2 by PTh, the photovoltaic performance of the PTh-sensitized solar cell was studied.

PTh-sensitized solar cell was fabricated by sandwiching the sensitized TiO_2 electrode with a platinum foil counter electrode. The redox electrolyte containing tetrabutyl ammonium iodide (TBAI) (0.5 mol/L)/I_2 (0.05 mol/L) in a mixture of propylene carbonate (PC, Acros) and ethylene carbonate (EC, Acros) (Volume ratio: 1∶3) was filled between the two electrodes.

The photocurrent-voltage curve of PTh-sensitized solar cell is illustrated in Figure 7, curve 1. As a result, the illuminated cell showed a short-circuit current density (I_{sc}) of 3.08 mA/cm^2 with an open circuit voltage (V_{oc}) of 511 mV under the irradiance of 100 mW/cm^2. The fill factor (FF) and the overall efficiency (η) of the DSSC was 0.57% and 0.9% respectively.

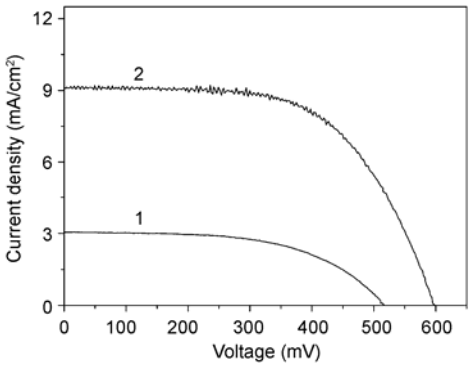

Figure 7 I-V characteristics of PTh-sensitized solar cell (curve 1) and N3-sensitized solar cell (curve 2). (Electrolyte: tetrabutyl ammonium iodide (TBAI) (0.5 mol/L)/I_2(0.05 mol/L) in a mixture of PC and EC (1∶3, *v*/*v*)).

In the same experimental conditions, we also measured N3-sensitized solar cell, the detailed parameters are listed in Table 2.

Table 2 Comparison of the solar cells parameters sensitized by PTh and N3 dyes

Sample	I_{sc} (mA cm^{-2})	V_{oc} (mV)	*FF*	η(%)
PTh-sensitized solar cell	3.08	511	0.57	0.90
N3-sensitized solar cell	9.08	598	0.61	3.29

Another important parameter associated with dye-sensitized solar cell is the monochromatic current yield (or incident monochromatic photon-to-current conversion efficiency, IPCE), which is expressed in terms of the light harvesting efficiency (LHE), the quantum yield of charge injection ϕ_{inj}, and the efficiency of collecting the injected charge at the back contact (η_c)[16].

$$IPCE(\lambda)=LHE(\lambda)\phi_{inj}\eta_c. \quad (11)$$

The light harvesting efficiency was given by

$$LHE(\lambda)=1-10^{-\Gamma\sigma(\lambda)}, \quad (12)$$

where Γ is the number of moles of sensitizer per square centimeter of projected surface area of the film and σ is the absorption cross section in units of cm^2/mol obtained from the decadic adsorption coefficient (units of (mol/L)$^{-1}$/cm) by multiplication with 1000 cm^3/L.

The surface concentration of PTh is about 2.0×10^{-9} mol/cm^2 which is smaller than N3 (1.3×10^{-7} mol/cm^2).

And the reason is that the molecular size of PTh is relatively large. The absorption cross section of PTh is 2.5×10^8 cm^2/mol, so the light harvesting efficiency is 68% at the absorption maximum of the sensitizer according to eq. (12). We suppose that η_c is nearly equal to 1 on the assumption that the injected electrons can percolate without significant loss through the network of interconnected particles present in the nanocrystalline TiO_2 film. According to eq. (11), the monochromatic current yield is around 47%, which is smaller than that of N3. So this is also the main reason for the relatively low overall efficiency.

The important dynamics of redox processes involved in the conversion of light to electric power by dye-sensitized solar cells are electron injection and dye regeneration. Cyclic voltammetry measurement was made to study the PTh dye regeneration reaction ($2PTh^+ +3I^- \rightarrow 2PTh+I_3^-$) at the nanocrystalline TiO_2/electrolyte interface. Figure 8 depicts the cyclic voltammograms measured in electrolyte under the scanning range of 0—1.2 V. The voltammogram shows the cathodic peak corresponding to the reduction of oxidized PTh dye by iodide at +0.97 V with cathodic peak current of 1.69 μA. The anodic peak cannot be observed in this scanning range indicating the irreversible behavior of this electrochemical reaction at PTh-coated FTO electrode. On the basis of the above results, it is suggested that an interfacial charge transfer reaction occurred and the PTh dye was regenerated.

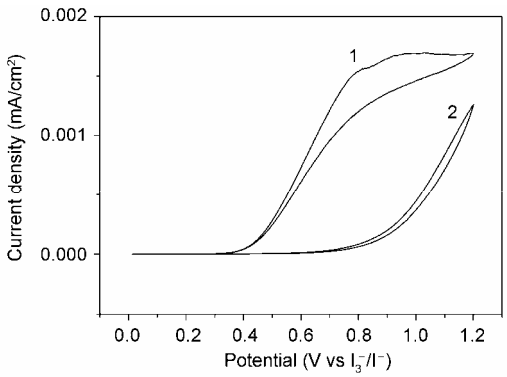

Figure 8 Cyclic voltammograms of PTh-coated FTO electrode 1 and blank FTO glass 2 measured in the electrolyte containing 0.5 mol/L TBAI, 0.05 mol/L iodine in EC/PC mixed solvent (EC:PC = 3:1, *v*/*v*).

3 Conclusions

UV-vis absorption and fluorescence spectroscopy was employed to investigate the interaction of Poly(3-{2-[4-(2-ethylhexyloxy)-phenyl]-vinyl}-2,2′-bithiophene) with nanocrystalline TiO_2. The fluorescence emission of the PTh can be efficiently quenched by TiO_2 nanoparticles owing to charge injection from the excited singlet state of PTh to the conduction band of the TiO_2 particles. According to fluorescence lifetime measurement, the rate constant of electron transfer (K_{et}) is 4.24×10^9 s^{-1}. PTh as an potential photosensitizer in the visible region was used to photosensitize nanocrystalline TiO_2 electrode of DSSC, and a considerable conversion efficiency was obtained. However, the performance of PTh sensitizer was not as good as N3 dye, and the main reasons are as follows: Firstly, the concentration of PTh adsorbed on TiO_2 surface was low because the molecule size of PTh was relatively large and the PTh sensitizer had no polar functional group. Besides low surface concentration of PTh, the relatively small rate constant of electron transfer was another reason. The LUMO energy level of PTh (–2.9 eV) was higher than that of N3 dye (–3.53 eV)[17], so the energy level was not the reason to bring about the small K_{et}. The small K_{et} was probably associated with that the PTh had no carboxylic groups unlike Ru polypyridyl complex sensitizer and the variation in the solvent environment. Although the efficiency of the solar cell sensitized by PTh was not high, there were large improving potentials such as visible absorption, and structure of molecule. For better usage in DSSC, we are now trying to anchoring polar functional group such as carboxylic group in the molecular of PTh.

1 Reagen B O, Grätzel M. A Low-cost, high-efficiency solar cell based on dye-sensitized colloidal TiO_2 films. Nature, 1991, 353(6346): 737—740[DOI]

2 Hagfeldt A, Grätzel M. Molecular photovoltaics. Acc Chem Res, 2000, 33(5): 269—277[DOI]

3 Grätzel M. Conversion of sunlight to electric power by nanocrystalline dye-sensitized solar cells. J Photochem Photobiol A: Chem, 2004, 164(1-3): 3—14

4 Nazeeruddin M K, Péchy P, Renouard T, et al. Engineering of efficient panchromatic sensitizers for nanocrystalline TiO_2-based solar cells. J Am Chem Soc, 2001, 123(8): 1613—1624[DOI]

5 Mcullough R D. The chemistry of conducting polythiophenes. Adv Mater, 1998, 10(2): 93—116[DOI]

6 Niemi V M, Knuuttila P, Österholm J E. polymerization of 3-alkylthiophenes with $FeCl_3$. Polymer, 1992, 33(7): 1559—1562[DOI]

7 Hou J, Tan Z, Yan Y, et al. Synthesis and photovoltaic properties of

two-dimensional conjugated polythiophenes with Bi(thienylenevinylene) side chains. J Am Chem Soc, 2006, 128(14): 4911—4916[DOI]
8 Hou J, Yang C, He C. Poly[3-(5-octyl-thienylene-vinyl)-thiophene]: A side-chain conjugated polymer with very broad absorption band. Chem Commun, 2006, (8): 871—873[DOI]
9 Ma W, Yang C, Gong X, et al. Thermally stable, efficient polymer solar cells with nanoscale control of the interpentrating network morphology. Adv Funct Mater, 2005, 15(10): 1617—1622[DOI]
10 Zhan X, Tan Z, Domercq B, et al. A high-mobility electron-transport polymer with broad absorption and its use in field-effect transistors and all-polymer solar cells. J Am Chem Soc, 2007, 129(23): 7246—7247[DOI]
11 Blom P W M, Mihailetchi V D, Koster L J A, et al. Device physics of polymer: Fullerene bulk heterojunction solar cells. Adv Mater, 2007, 19(12): 1551—1566[DOI]
12 Thompson B C, Frëchet J M J. Polymer-fullerene composite solar cells. Angew Chem Int Ed, 2008, 47(1): 58—77[DOI]
13 Hou J, Huo L, He C, et al. Synthesis and absorption spectra of poly(3-(phenylenevinyl)thiophene) with conjugated side chains. Macromolecules, 2006, 39(2): 594—603[DOI]
14 Kamat P V. Photoelectrochemistry in particulate systems. 9. Photosensitized reduction in a colloidal titania system using anthracene-9- carboxylate as the sensitizer. J Phys Chem, 1989, 93(2): 859—864[DOI]
15 Kamat P V. Photochemistry on nonreactive and reactive (semiconductor) surfaces. Chem Rev, 1993, 93(1): 267—300[DOI]
16 Nazeeruddin M K, Kay A, Rodicio I, et al. Conversion of light to electricity by cis-X_2bis(2,2′-bipyridyl-4,4′-dicarboxylate) ruthenium (II) charge-transfer sensitizers (X=Cl^-, Br^-, I^-, CN^-, and SCN^-) on nanocrystalline titanium dioxide electrodes. J Am Chem Soc, 1993, 115(14): 6382—6390[DOI]
17 Seiichi S, Shogo M, Sinya S, et al. Photoelectrochemical characteristics of cells with dyed and undyed nanoporous p-type semiconductor CuO electrodes. J Photochem Photobiol A: Chem, 2008, 194(2-3): 143—147